Inflammatory bone loss associated with MFG-E8 deficiency is rescued by teriparatide

Megan N. Michalski,* Anna L. Seydel,* Erica M. Siismets,* Laura E. Zweifler,* Amy J. Koh,*
Benjamin P. Sinder,* J. Ignacio Aguirre,† Kamran Atabai,‡ Hernan Roca,* and Laurie K. McCauley*,§,1

*Department of Periodontics and Oral Medicine, University of Michigan School of Dentistry, and §Department of Pathology, University of Michigan Medical School, University of Michigan, Ann Arbor, Michigan, USA; †Department of Physiological Sciences, College of Veterinary Medicine, University of Florida, Gainesville, Florida, USA; and ‡Department of Medicine, Cardiovascular Research Institute, University of California, San Francisco, San Francisco, California, USA

ABSTRACT: A prolonged increase in proinflammatory cytokines is associated with osteoporotic and autoimmune bone loss and, conversely, anti-inflammatory pathways are associated with protection against bone loss. Milk fat globule-epidermal growth factor (MFG-E)-8 is a glycoprotein that is proresolving, regulates apoptotic cell clearance, and has been linked to autoimmune disease and skeletal homeostasis. The role of MFG-E8 in the young *vs.* adult skeleton was determined in mice deficient in MFG-E8 (KO). *In vivo*, trabecular bone was similar in MFG-E8KO and wild-type (WT) mice at 6 and 16 wk, whereas 22 wk adult MFG-E8KO mice displayed significantly reduced trabecular BV/TV. The number of osteoclasts per bone surface was increased in 22-wk MFG-E8 KO *vs.* WT mice, and recombinant murine MFG-E8 decreased the number and size of osteoclasts *in vitro*. Adult MFG-E8KO spleen weight:body weight was increased compared with WT, and flow cytometric analysis showed significantly increased myeloid-derived suppressor cells (CD11b^{hi}GR-1$^+$) and neutrophils (CD11b^{hi}Ly6G$^+$) in MFG-E8KO bone marrow, suggesting an inflammatory phenotype. PTH-treated MFG-E8KO mice showed a greater anabolic response (+124% BV/TV) than observed in PTH-treated WT mice (+64% BV/TV). These data give insight into the role of MFG-E8 in the adult skeleton and suggest that anabolic PTH may be a valuable therapeutic approach for autoimmune-associated skeletal disease.—Michalski, M. N., Seydel, A. L., Siismets, E. M., Zweifler, L. E., Koh, A. J., Sinder, B. P., Aguirre, J. I., Atabai, K., Roca, H., McCauley, L. K. Inflammatory bone loss associated with MFG-E8 deficiency is rescued by teriparatide. FASEB J. 32, 3730–3741 (2018). www.fasebj.org

KEY WORDS: osteoporosis · osteoclasts · PTH · immune cells

Milk fat globule epidermal growth factor (MFG-E)-8 is a secreted glycoprotein that was first identified in the mammary gland and subsequently studied in many other tissues (1–4). One of the most prominent functions of MFG-E8 is to act as a bridge between apoptotic and phagocytic cells, thus coordinating the engulfment of apoptotic cells, a process termed efferocytosis (5–8). MFG-E8 has also been linked to other functions in the body, including collagen clearance by lung alveolar macrophages (2), angiogenesis in cutaneous wound healing (9), phagocytosis in the retina (4), and polarization of tumor-associated macrophages (10). MFG-E8 is an important regulator of the inflammatory response, and mice deficient in MFG-E8 have inflammatory phenotypes, including intestinal colitis and systemic lupus erythematosus (SLE)–like symptoms (6, 11, 12). In humans, a genetic polymorphism of MFG-E8 correlated significantly with human SLE (13).

A role of MFG-E8 has recently emerged in bone as a positive regulator of bone turnover (14) and a protective factor against rheumatoid arthritis (15). MFG-E8–deficient mice had reduced bone mass and accelerated bone loss in a ligature-induced periodontitis model (16), yet the exact functional role of MFG-E8 in bone turnover is still unclear. MFG-E8 expression in many tissues leads to an anti-inflammatory response, resulting in the reduction of

proinflammatory factors such as TNF-α, IL-1β, and IL-6 (17). MFG-E8 has been shown to decrease inflammation and improve survival in a model of rat sepsis (18) and MFG-E8 enhances wound healing in diabetic mice by decreasing inflammation and increasing proresolving factors (19). Although contributions of inflammatory cytokines to osteoporosis have been well characterized, the roles of anti-inflammatory or resolving cytokines are studied less. Because of the resolving nature of MFG-E8, it has been hypothesized that it plays a role in inflammatory bone loss.

Teriparatide [human parathyroid hormone; (h) PTH(1–34)] is a U.S. Food and Drug Administration (FDA)-approved injectable anabolic therapeutic used to treat osteoporosis. It is well established that intermittent PTH increases bone mass, bone formation, and bone turnover, but the exact mechanisms regulating these effects are unknown. Direct treatment of osteoblasts *in vitro* with PTH does not stimulate an anabolic response, suggesting that other cell types in the bone marrow microenvironment are critical to *in vivo* PTH anabolic actions (20, 21). PTH has been shown to alter marrow inflammatory cells, including neutrophils and macrophages (22, 23), the latter of which strongly regulates bone mass (24). Although PTH has been used to increase bone, the focus of therapeutic potential in rescuing inflammation-induced bone loss is less understood. In addition, therapeutic interventions to rescue MFG-E8-associated bone loss have not been investigated. It is hypothesized that MFG-E8 deficiency increases inflammation leading to bone loss rescued by PTH treatment. The purpose of the present study was to assess the role of inflammation in MFG-E8–associated bone loss and to investigate an anabolic therapeutic intervention in MFG-E8–deficient mice.

MATERIALS AND METHODS

Animals

All mice were maintained in accordance with institutional animal care and use guidelines, and experimental protocols were approved by the Institutional Animal Care and Use Committee of the University of Michigan. MFG-E8–deficient knockout (KO) mice were originally created by using a gene trap vector and backcrossed onto a C57BL/6 background [wild-type (WT) controls] (1, 2). Mice were housed at a density of 3–5 mice per cage in specific pathogen-free conditions and fed a standard diet of Purina 5001 chow (Purina, Indianapolis, IN, USA). For *in vivo* experiments, mice were given IDs for blinded assessment during treatment and subsequent analyses. Female mice were used for *in vitro* or *in vivo* experiments at ages 6 wk (WT, $n = 13$; KO, $n = 11$), 16 wk (WT, $n = 9$; KO, $n = 8$), and 22 wk (WT, $n = 10$; KO, $n = 10$), and male mice were analyzed at 22 wk (WT, $n = 6$; KO, $n = 5$). To test the anabolic effect of intermittent PTH, 16-wk-old female and male KO and WT mice were randomized into treatment groups and treated daily with recombinant human PTH(1–34) (50 μg/kg, s.c.; Bachem, Torrance, CA, USA) or vehicle (Veh; 0.9% saline, s.c.) for 6 wk (female: WT Veh, $n = 10$; WT PTH, $n = 11$; KO Veh, $n = 10$; and KO PTH, $n = 10$; and male: WT Veh, $n = 6$; WT PTH, $n = 5$; KO veh, $n = 7$; and KO PTH, $n = 6$), according to previously published dosage regimens (20, 21). MFG-E8 KO mice were crossed with Mertk KO mice (The Jackson Laboratory, Bar Harbor, ME, USA) to create double MFG-E8/Mertk KO mice (dKO). Mertk is an efferocytic receptor on macrophages. Skeletal phenotypes were assessed in female mice at 6 (WT, $n = 10$; dKO, $n = 11$), 16 (WT, $n = 9$; KO, $n = 7$), and 22 wk (WT, $n = 6$; KO, $n = 6$), and mice were treated in the same manner as KO mice with PTH (WT Veh, $n = 6$; WT PTH, $n = 9$; KO Veh, $n = 6$; and KO PTH $n = 9$). No adverse events were noted in the experimental groups.

Complete blood counts

Blood was collected at the time of euthanasia *via* intracardiac puncture from mice at ages 6, 16, and 22 wk, in Microtainer Tubes with K2E (K$_2$EDTA; BD, Franklin Lakes, NJ, USA), and analyzed for complete blood count with differential.

Serum ELISA

Mice underwent food and water restriction for 6 h before serum collection. Blood was harvested as above, and placed in non-EDTA–containing microcentrifuge tubes, allowed to coagulate for at least 1 h at room temperature, and spun down at 8000 rpm for 10 min, and liquid serum was collected into new microcentrifuge tubes. Samples were stored at $-20°C$ until use. Enzyme immunoassays were used to measure the serum concentrations of tartrate-resistant acid phosphatase form 5b (TRAcP 5b), propeptide of type I procollagen (P1NP), and C-telopeptide of type I collagen (CTX-I), according to the manufacturer's instructions (Immuno Diagnostic Systems, Tyne and Wear, United Kingdom) and measured on an EZ Read 400 Microplate Reader (Biochrom, Holliston, MA, USA).

Fluorescence-activated cell sorting analysis

Bone marrow was isolated from the femur by flushing into fluorescence-activated cell sorting (FACS) buffer [1× PBS with 2% fetal bovine serum (FBS) and 0.5 mM EDTA], and 10^6 cells were stained with anti-mouse F4/80 [allophycocyanin (APC), Clone A3-1; Abcam, Cambridge, United Kingdom] and anti-mouse CD68 [fluorescein isothiocyanate (FITC), Clone FA-11], anti-mouse CD11b (APC, M1/70), anti-mouse Gr-1 (FITC, RB6-8C5), and anti-mouse Ly6G (FITC, 1A8; all from BioLegend, San Diego, CA, USA). Isotype controls were used to confirm antibody specificity. FACS analysis was performed with a FACS Aria III (BD).

Microcomputed tomography

Tibiae were harvested from 6-, 16-, and 22-wk-old mice and fixed in 10% neutral buffered formalin (NBF) for 24–48 h at 4°C, and stored in 70% ethanol. The bones were scanned by microcomputed tomography (μCT) at a 12-μm voxel size (μCT-100; Scanco, Wayne, PA, USA) (22), according to established guidelines (25). Trabecular bone was measured starting 360 μm distal to the top of the proximal tibial growth plate and extending 600 μm distally with a threshold of 180 mg/cm^3. Trabecular bone morphometric values analyzed included bone volume/total volume (BV/TV), trabecular number (Tb.N), trabecular thickness (Tb.Th), trabecular spacing (Tb.Sp), and trabecular bone mineral density (Tb.BMD). Cortical bone was measured starting 3 mm proximal to the tibia–fibula junction and extended 360 μm, with a threshold of 280 mg/cm^3. Cortical bone morphometric values analyzed included Tt.V, Ct.V, Ct.V/Tt.V, Ct.Th., and BMD.

TUNEL staining

Spleens and tibiae were fixed in 10% NBF for 24–48 h at 4°C. Tibiae were decalcified in 14% EDTA for 10–14 d. Spleens and

tibiae were processed, embedded in paraffin, and sectioned at 5 μm. Sections were stained for TUNEL+ cells (*In Situ* Cell Death Detection Kit, TMR red; Roche, Mannheim, Germany). TUNEL+ cells were quantified in the white pulp of the spleen and in the bone marrow of 22-wk-old WT and KO mice.

Static histomorphometry

Tibiae were fixed in 10% NBF for 24–48 h at 4°C, decalcified in 14% EDTA for 10–14 d, embedded in paraffin, and sectioned at 5 μm. A central slice of the proximal tibiae was stained with hematoxylin and eosin (H&E) or tartrate-resistant acid phosphatase (TRAP kit 387A; MilliporeSigma, St. Louis, MO, USA), and bone morphometry (bone area:total area) and osteoclast quantification were performed as described in Sinder *et al.* (26), according to standards set by the American Society of Bone Mineral Research (27). The region of interest was manually defined, beginning 200 μm distal to the most distal aspect of the proximal growth plate and extending 1200 μm distally.

Dynamic histomorphometry

Five and 2 d before euthanasia, the fluorochrome calcein was administered (30 mg/kg, i.p.; MilliporeSigma), which is incorporated into actively forming bone. Tibiae were harvested and fixed in 10% NBF for 24–48 h and stored in 70% ethanol. Undecalcified tibiae were embedded in methylmethacrylate, sectioned (8 μm), and dual-labeled surfaces quantified (28). The bone formation rate (BFR/BS) and mineral apposition rate (MAR) were analyzed.

In vitro osteoclast assays

Bone marrow from 6-wk-old KO or WT mice was extracted into 100 mm dishes in complete α-MEM [10% FBS, penicillin/streptomycin (pen/strep), and glutamine]. The following day, nonattached cells were replated on Petri dishes and treated with murine M-CSF (30 ng/ml; Thermo Fisher Scientific, Waltham, MA, USA) for 4–5 d. Cells were then split with 10 μM EDTA in ice-cold PBS and replated at 60,000/cm² in 48- or 96-well plates with M-CSF (30 ng/ml) and murine receptor activator of NF-κ B-ligand (RANKL; 50 ng/ml; PeproTech, Rocky Hill, NJ, USA). Osteoclastic cells were identified *via* TRAP staining (387A Kit; MilliporeSigma) or seeded onto Corning Osteoassay plates (MilliporeSigma) to measure resorptive functional activity. Osteoclast assays were performed as above with bone marrow from 22-wk-old WT mice. At the time of osteoclast differentiation induction with RANKL, cell cultures were treated with rmMFG-E8 (500 ng/ml; R&D Systems, Minneapolis, MN, USA) or bovine serum albumin (BSA) control (500 ng/ml; MilliporeSigma), according to published methods (14). Cultures were stained for TRAP and quantified.

Efferocytosis

Bone marrow macrophages were assessed for efferocytic capacity of apoptotic bone marrow stromal cells (BMSCs) or apoptotic thymocytes. Bone marrow from 6- or 22-wk-old WT or KO mice was harvested and cultured in macrophage differentiation medium (α-MEM, 10% FBS, pen/strep, glutamine, and 30 ng/ml M-CSF) for 7 d and replated in 6-well plates at a density of 1.5×10^6/well. BMSCs were harvested from 6- to 8-wk-old KO and WT mice *via* bone marrow flush and cultured in α-MEM (20% FBS, pen/strep, and glutamine)

containing 10 nM dexamethasone (MilliporeSigma). BMSCs were grown to confluence, dissociated from tissue culture plates with 0.25% trypsin-EDTA, and resuspended in 1× PBS. BMSCs were stained with the Invitrogen CellTrace CFSE Cell Proliferation Kit (2 μM; Thermo Fisher Scientific). Apoptosis was induced by exposure to UV light for 30 min, and cells were allowed to recover at 37°C for 2 h. The thymus was dissected from 6- to 10-wk-old KO or WT mice in ice-cold 1× PBS and pressed though a 70 μm cell strainer. Red blood cells were lysed with 1× ammonium chloride potassium (ACK), and resuspended in complete α-MEM plus 0.1 μM dexamethasone. Thymocytes were incubated at 37°C for 16 h to induce apoptosis, then stained with succinimidyl ester (SE) (20 ng/ml; pHrodo Red; Thermo Fisher Scientific) (29). Apoptotic BMSCs and thymocytes were counted *via* trypan blue exclusion and resulted in 80–95% apoptosis. Apoptotic cells (BMSCs or thymocytes) were cultured with macrophages at a 1:1 ratio in plain α-MEM for 2 h, fixed in 1% PFA, and stained for F4/80-APC (A3-1; Abcam). Efferocytosis was measured *via* flow cytometric analysis for double labeling APC-carbofluorescein SE (engulfed apoptotic BMSCs) or APC-pHrodo-SE (engulfed thymocytes). Phagocytosis by bone marrow macrophages was measured using pHrodo Green *E. coli* BioParticles (Thermo Fisher Scientific) and imaged using IncuCyte Live-Cell Analysis (Sartorius, Ann Arbor, MI).

Statistical analysis

All statistical analyses were performed with Prism 7 software (GraphPad, La Jolla, CA, USA). Statistical analyses were performed by unpaired Student's *t* test to compare 2 groups or ANOVA with the least-significant difference *post hoc* test, to compare 3 or more groups (PTH and vehicle treatments) with a significance of $P < 0.05$. Data are means ± SEM.

RESULTS

MFG-E8 deficiency leads to reduced bone mass in adult mice

The skeletal phenotypes of female MFG-E8–deficient mice were assessed at 6, 16, and 22 wk and compared with those of age-matched WT controls. At 6 wk of age, MFG-E8 and WT mice had similar trabecular BV/TV (**Fig. 1*A*, *B***) and Ct.V/Tt.V (Fig. 1*C*). With age, MFG-E8–deficient mice had lower bone mass relative to WT, with significantly decreased trabecular BV/TV at 22 wk and significantly reduced cortical bone at 16 and 22 wk. Serum ELISAs for bone formation (Fig. 1*D*) and resorptive markers (Fig. 1*E*, *F*) showed similar trends in KO and WT mice with age. Serum TRAcP 5b, a marker reflecting the number of osteoclasts, was decreased in MFG-E8 KO mice at 22 wk of age compared with WT. In contrast, CTX-I, a marker of osteoclast resorptive activity was increased in MFG-E8 KO mice at 22 wk *vs.* WT controls.

Further trabecular bone analysis of the tibiae confirmed that 22-wk-old KO mice had significantly decreased trabecular BV/TV (−23%; **Fig. 2*A***), unchanged Tb.Th. (−4%; Fig. 2*B*), unchanged Tb.N (−8%; Fig. 2*C*), unchanged Tb. Sp (+8%; Fig. 2*D*), and decreased trabecular BMD (−22%; Fig. 2*E*) compared with WT control mice. Cortical volume fraction and Ct.Th. were significantly decreased 4 and 9%,
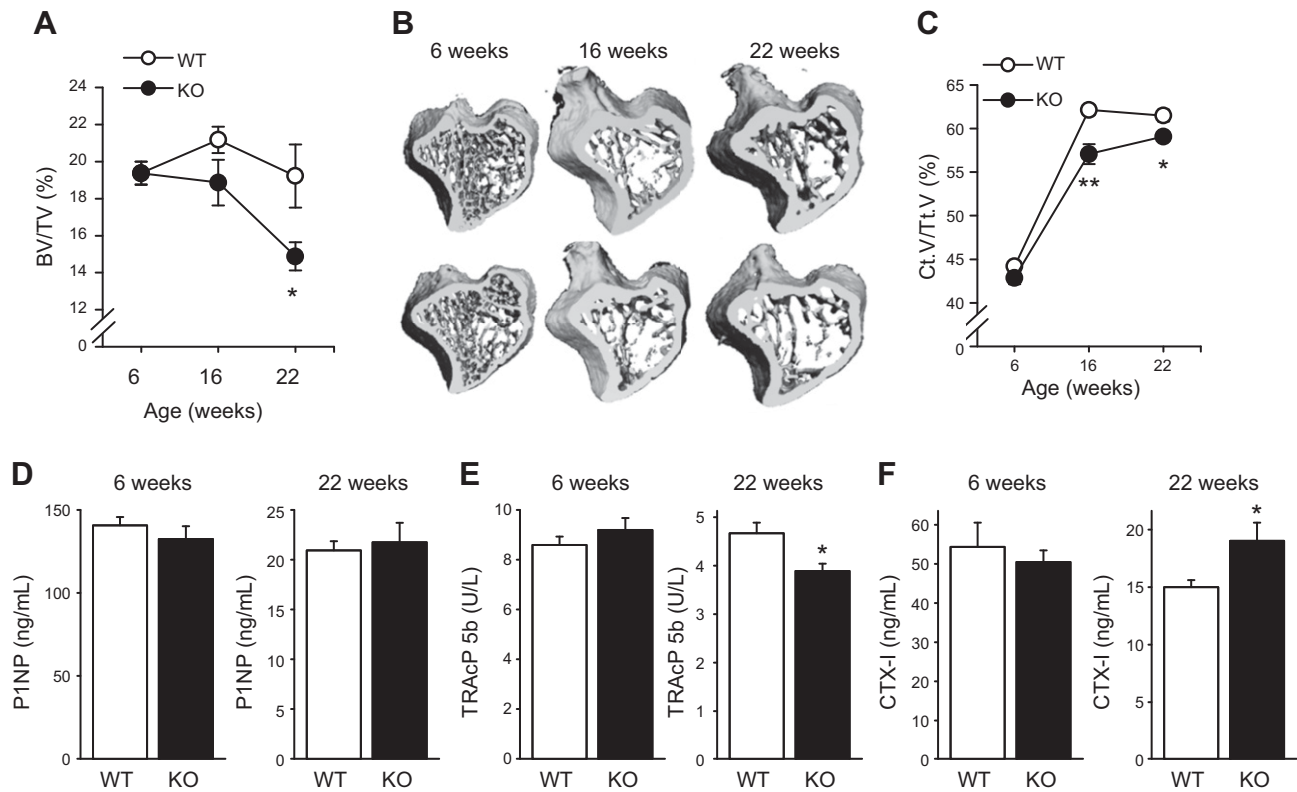
Figure 1. Adult MFG-E8 KO mice have reduced bone mass. *A–C*) Tibiae harvested from 6-, 16-, and 22-wk-old female MFG-E8 KO and WT mice were analyzed for trabecular BV/TV (*A*, *B*) and Ct.V/Tt.V (*B*, *C*) by µCT. *D–F*) The serum bone formation marker P1NP and serum resorptive markers (*D*), TRAcP 5b (*E*), and CTX-I (*F*) were measured *via* ELISA at the time of euthanasia. Data are mean ± SEM (*n* = 8–13/group). *$P < 0.05$, **$P < 0.01$.

respectively, in KO *vs.* WT mice (Fig. 2*F*, *G*). Dynamic histomorphometry was performed in mice at 22 wk of age, with no significant changes observed in BFR/BS or MAR between KO and WT mice (Fig. 2 *H*, *I*).

MFG-E8 deficiency is associated with increased osteoclasts

The number of osteoclasts per bone surface (N.Oc/BS) was increased in 22-wk-old KO *vs.* WT mice (**Fig. 3***A*). To better understand the cellular contributions to the skeletal phenotype seen in the MFG-E8–deficient mice, a series of *in vitro* assays were performed. *In vitro* osteoclast assays from 6-wk-old mice revealed no significant alterations in osteoclast differentiation or resorptive capacity between WT and KO mice (Fig. 3*B*). Osteoclasts from 22-wk-old WT mice were cultured with recombinant murine (rm)MFG-E8 or vehicle (BSA), stained for TRAP, and quantified. Treatment with rmMFG-E8 significantly reduced the number and size of osteoclasts (−82%, Fig. 3*C*).

Loss of MFG-E8 results in altered immunologic profile in spleen and bone marrow

To evaluate the immunologic impact of MFG-E8, spleens were harvested and weighed from 22-wk-old KO and WT mice. KO mice had significantly increased spleen weight

per body weight compared to WT mice (**Fig. 4***A*). Spleens and tibiae were fixed, embedded in paraffin, sectioned, and stained for TUNEL+ cells reflecting cell death. TUNEL+ cells were increased in the white pulp of spleens from 22-wk-old KO mice compared to WT (Fig. 4*B*), which implies a site-specific efferocytic function of MFG-E8, because TUNEL+ cells were unchanged in the bone marrow of 16- and 22-wk-old KO and WT mice (Fig. 4*C*). This finding suggests that apoptotic cell clearance in the marrow may be facilitated *via* other efferocytic pathways. *In vitro* efferocytosis studies were performed to assess the effect of MFG-E8 deficiency on bone marrow macrophage engulfment of apoptotic cells. No significant alterations in engulfment of apoptotic BMSCs or thymocytes were seen *in vitro* (data not shown). Phagocytosis was measured with the bioparticle pHrodo, which fluoresces when engulfed. Uptake of pHrodo was decreased by KO bone marrow macrophages compared to WT (Fig. 4*D*). This result suggests that, although the KO bone marrow macrophages may not have an efferocytic phenotype, phagocytosis of particles was compromised, reflecting altered macrophage function. FACS analysis of bone marrow populations revealed that KO mice had significantly increased neutrophils (CD11b^hiLy6G+; Fig. 4*E*) and myeloid-derived suppressor cells (MDSCs, CD11b^hiGr-1+; Fig. 4*F*) *vs.* WT mice. F4/80+ (murine macrophages) and CD68+ (macrophage and dendritic cells) populations were not changed in KO mice *vs.* WT (data not shown).
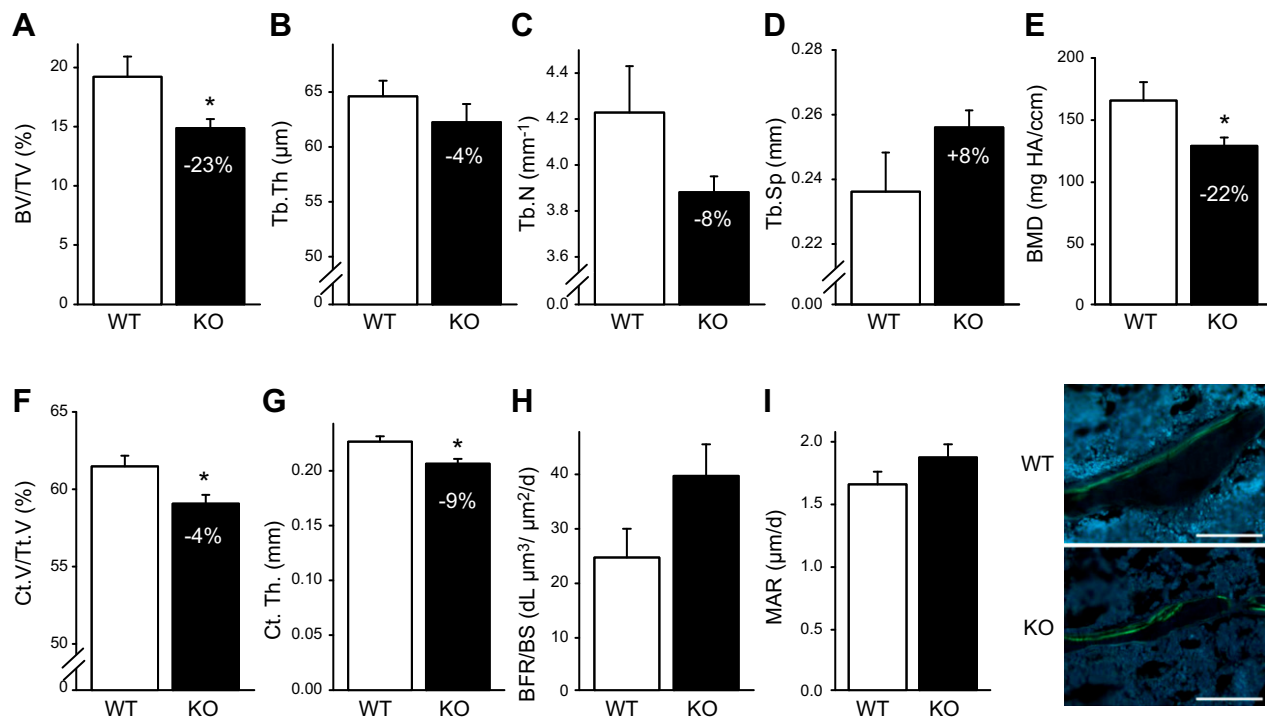
Figure 2. Adult (22 wk) KO mice have reduced bone mass and increased the number of osteoclasts. *A–E*) Tibiae were harvested from female 22-wk-old WT and KO mice, and trabecular parameters were quantified *via* μCT. KO mice displayed significantly reduced trabecular BV/TV (*A*), Tb.N (*C*), and Tb.BMD (*E*). Tb.Th (*B*) and Tb.Sp (*D*) were not significantly different in WT and KO mice. *F, G*) Cortical bone was measured in the midshaft of the tibiae of 22-wk-old WT and KO mice. KO mice had reduced Ct.V/Tt.V (*F*) and Ct.Th. (*G*) compared to WT control mice. *H, I*) Calcein was administered (30 mg/g, i.p.) 5 and 2 d before euthanasia to measure active bone formation. Dynamic histomorphometric analyses were performed in the cancellous bone of the proximal tibia. Sections were analyzed for BFR/BS (*H*) and MAR (*I*). No significant differences were seen between WT and KO mice. Data are mean ± SEM (*n* = 6–11/group). *$P < 0.05$. Scale bars, 100 μm.

MFG-E8 KO mice have greater increases in BV/TV in response to intermittent PTH treatment

Female MFG-E8 KO and WT mice (16 wk) were treated daily with PTH or vehicle for 6 wk (until 22 wk of age) to evaluate the therapeutic potential of a known anabolic bone agent (**Fig. 5***A*). All data are presented as treatment (PTH) over control (Veh). PTH increased spleen weight similarly in both WT and KO mice (treated:control >1.0; Fig. 5*B*). PTH did not alter the CD11b^hiLy6G+ populations in WT or KO mice, whereas PTH increased marrow CD11b^hiGr-1+ cells in WT, but not in KO, mice (Fig. 5*C*). Complete blood counts from WT and KO mice treated with vehicle or PTH showed that PTH treatment decreased the percentage of neutrophils in the peripheral blood of both WT and KO-treated mice (**Table 1**). Red blood cell mean corpuscular volume and hemoglobin were significantly increased in KO *vs.* WT mice, and PTH further increased these parameters in KO mice.

Adult mice treated with vehicle or PTH were assessed for skeletal phenotypes. Trabecular bone analysis of the tibia *via* μCT showed that both WT and KO mice responded to PTH treatment (treated:control, >1.0; Fig. 5*D–G*). KO mice showed a significantly greater anabolic response to PTH in BV/TV, Tb.N, and Tb.BMD than PTH-treated WT mice. KO and WT had similar cortical bone anabolic responses to PTH (Fig. 5*H, I*). Supplemental Table 1 provides the raw values for these μCT findings. Static

histomorphometry of tibiae showed an increased bone mass in both WT and KO mice in the proximal tibia (Fig. 5*J*). Although vehicle-treated (control) KO male mice (22 wk) did not display a statistically significant bone phenotype compared to vehicle-treated (control) WT (−10% BV/TV; $P = 0.26$), their response to PTH was augmented when compared to PTH-treated WT mice (WT +19% BV/TV, $P = 0.07$, *vs.* KO+49% BV/TV, $P < 0.05$).

In addition to the role of MFG-E8 in efferocytosis, Mertk is another key efferocytic receptor on macrophages. Therefore, MFG-E8/Mertk dKO mice were generated to assess the effect of the absence of another efferocytic pathway. The resulting skeletal phenotype of the dKO mice was similar to the MFG-E8KO phenotype (Supplemental Fig. 2*A, B*). dKO mice had a trend of decreasing bone with age and responded to PTH treatment to a greater extent than WT controls (Supplemental Fig. 2*C*). These data suggest Mertk deficiency does not alter the skeletal phenotype further *vs.* MFG-E8 deficiency alone.

MFG-E8 KO mice display increased osteoclast surface, rescued by PTH treatment

The serum formation marker P1NP and serum resorptive markers TRAcP 5b and CTX-I were all increased with PTH treatment in both KO and WT mice (**Fig. 6***A–C*). The
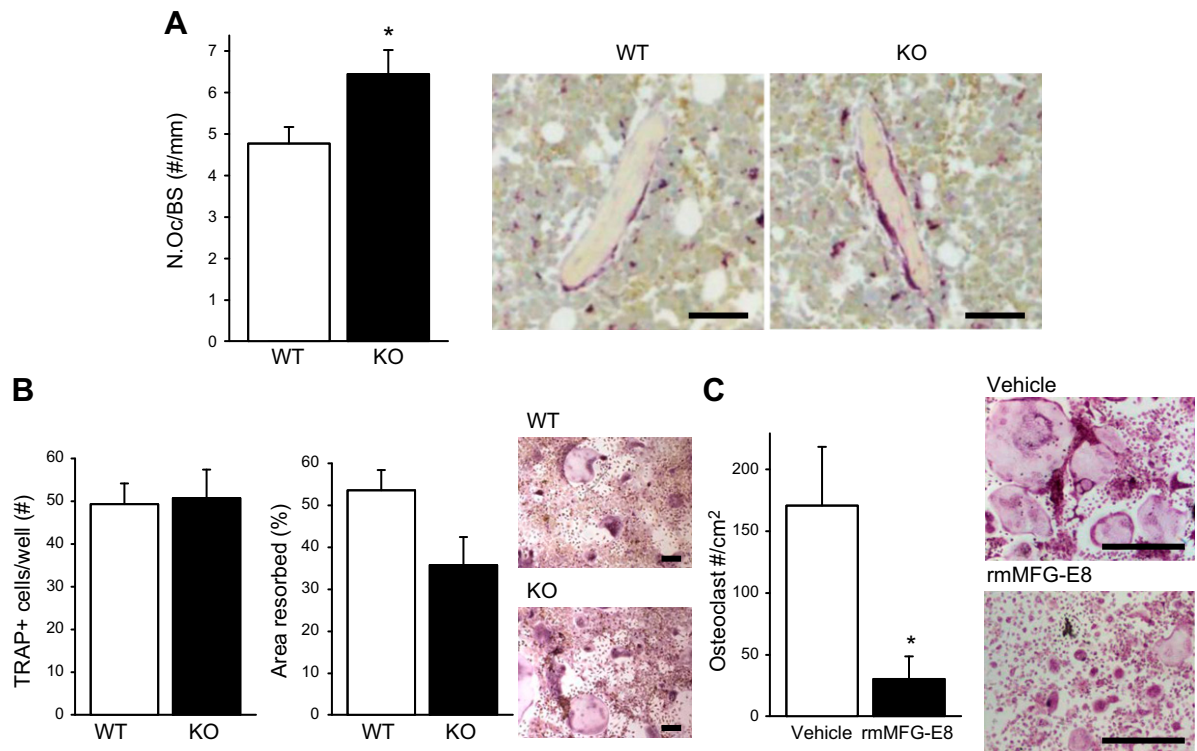
Figure 3. MFG-E8 regulates osteoclastogenesis. *A*) Paraffin-embedded tibiae were sectioned and stained for TRAP, a marker for osteoclasts. TRAP$^+$ multinucleated osteoclasts were quantified per bone surface (N.Oc/BS). Representative images on right. Scale bars, 50 μm. *B*) Osteoclasts were derived from 6-wk-old KO and WT mice. Osteoclast differentiation (TRAP staining) and resorptive activity were measured. Scale bar, 200 μm. *C*) Osteoclasts were derived from 22-wk-old mice and treated with vehicle (BSA control) or rmMFG-E8 (500 ng/ml), stained for TRAP and quantified. Data are mean ± SEM (*n* = 3/group repeated 2–3 times with similar results). Scale bars, 500 μm. *P < 0.05.

PTH-mediated increase in serum P1NP was significantly higher in KO *vs.* WT mice. BFR/BS and MAR were increased in with PTH treatment in both WT and KO mice (Fig. 6*D*, *E*). The increase in N.Oc/BS in KO mice compared with WT was reduced with PTH treatment in KO mice (Fig. 6*F*).

DISCUSSION

It is well accepted that chronic inflammation increases during the aging process, leading to the upregulation of proinflammatory mediators. Chronic increases in inflammatory cytokines are seen in postmenopausal osteoporosis, a disease with a pathology related to increased osteoclast differentiation and activity (30). The current study describes the contributions of MFG-E8 in the young and adult murine skeleton. MFG-E8 is a known antiinflammatory mediator. MFG-E8–deficient mice developed a skeletal phenotype that became apparent with age. At 16 wk of age, MFG-E8 KO mice showed a trend of decreased trabecular bone and significantly decreased cortical bone compared to WT and then displayed significantly decreased trabecular and cortical bone at 22 wk of age. These data suggest that MFG-E8 is a contributor to bone turnover in adult bone. A previous report of MFG-E8 contributions to bone showed decreased vertebral trabecular bone volume fraction in MFG-E8–

deficient mice as early as 6 wk of age (14) and may describe a location-specific effect. The difference in age at onset of an osteopenic phenotype between these 2 models may also represent differences in the development of the genetic models. The genetic model presented here was developed by inserting the pGT1-pfs gene trap vector in intron 7 of *Mfge8*, leading to protein degradation (1), whereas Sinningen *et al.* (14) used a KO model that was generated by replacing exons 2–6 of *Mfge8* with a neomycin resistance cassette (31). This finding suggests that disrupting the proper transcription of the gene may result in a more dramatic phenotype present at an earlier age, whereas the prevention of protein secretion results in a phenotype that becomes apparent with time.

Male KO mice did not have a significant reduction in trabecular BV/TV at 22 wk of age, whereas female mice displayed a significant reduction in bone. Sinningen *et al.* (14) also saw a reduced bone phenotype in female mice, suggesting a possible sex-specific phenotype; however, data describing the male phenotype were not presented. Given that MFG-E8 is highly expressed in mammary gland tissue and is important in mammary gland development and involution (1), it may be associated with hormonal controls related to sex steroids that in turn have a gender-specific effect on the skeleton. MFG-E8 deficiency is associated with autoimmune disease, and autoimmune disorders are more common in females than in males.
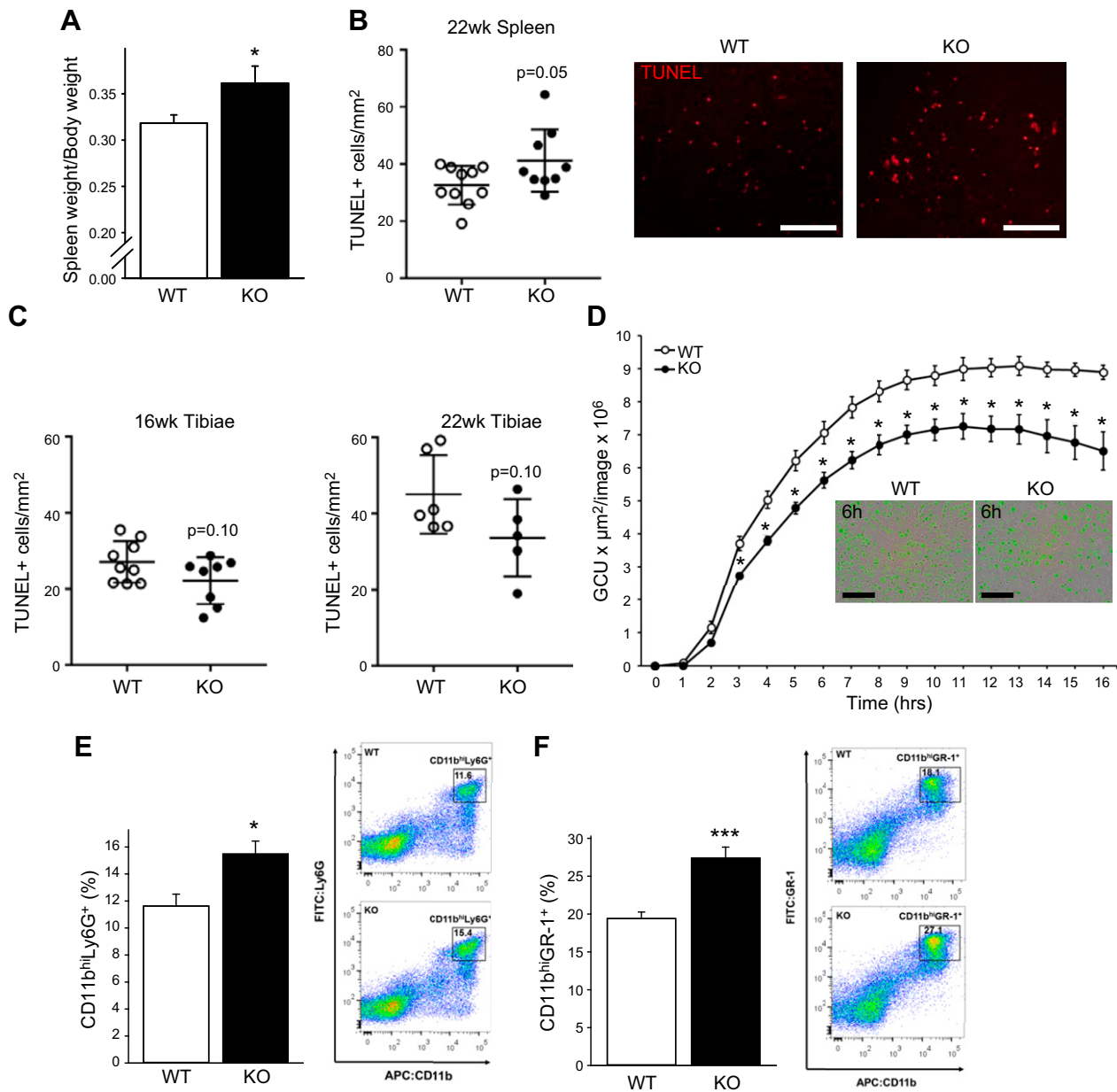
Figure 4. Adult MFG-E8 KO mice have increased spleen size and increased marrow neutrophils and myeloid cells. *A*) Spleens were harvested at the time of euthanasia from female 22-wk-old WT and KO mice, weighed, and compared to body weight (*n* = 10–11/group). *B, C*) Spleens and tibiae were processed, embedded in paraffin, sectioned, and stained for TUNEL⁺ cells, reflecting cell death. Scale bars, 100 μm. *D*) Uptake of pHrodo Green *E. coli* BioParticles conjugates by bone marrow macrophages. Scale bars, 200 μm. *E, F*) Marrow was flushed from femora of 22-wk-old female WT and KO mice and stained for flow cytometric analysis of CD11b^{hi}Ly6G$^+$ (neutrophils) and CD11b^{hi}Gr-1$^+$ (immature myeloid cells) populations. Data are means ± SEM (*n* = 6–8/group). *$P < 0.05$, ***$P < 0.001$.

Given the relationship between inflammation and osteoclast activation, we sought to identify whether the reduced bone phenotype in MFG-E8–deficient mice would correlate with an enhanced inflammatory environment. The reduced bone phenotype in MFG-E8 KO mice has been attributed to an increased in osteoclasts, *via* mechanisms that are not clearly delineated (16). In concert with an osteoclastic phenotype, administration of rmMFG-E8 protein to inflammation-induced periodontal bone defects decreased bone loss (16). An inflammatory phenotype has not been described in the bones of MFG-E8–deficient mice.

Adult MFG-E8 KO mouse spleen weights, bone marrow neutrophils, and MDSCs increased. These findings are consistent with an increased inflammatory phenotype. Increased spleen weight was seen in MFG-E8 KO at 40 wk of age (6) and MFG-E8 KO mice display signs of inflammation in other tissues (12). In the present study, MFG-E8 KO mice showed an increased in N.Oc/BS and increased serum CTX-I levels, consistent with an inflammation-induced osteoclastogenesis. This result may seem contrary to the serum ELISA studies that showed a decrease in serum TRAcP 5b but may be explained by the
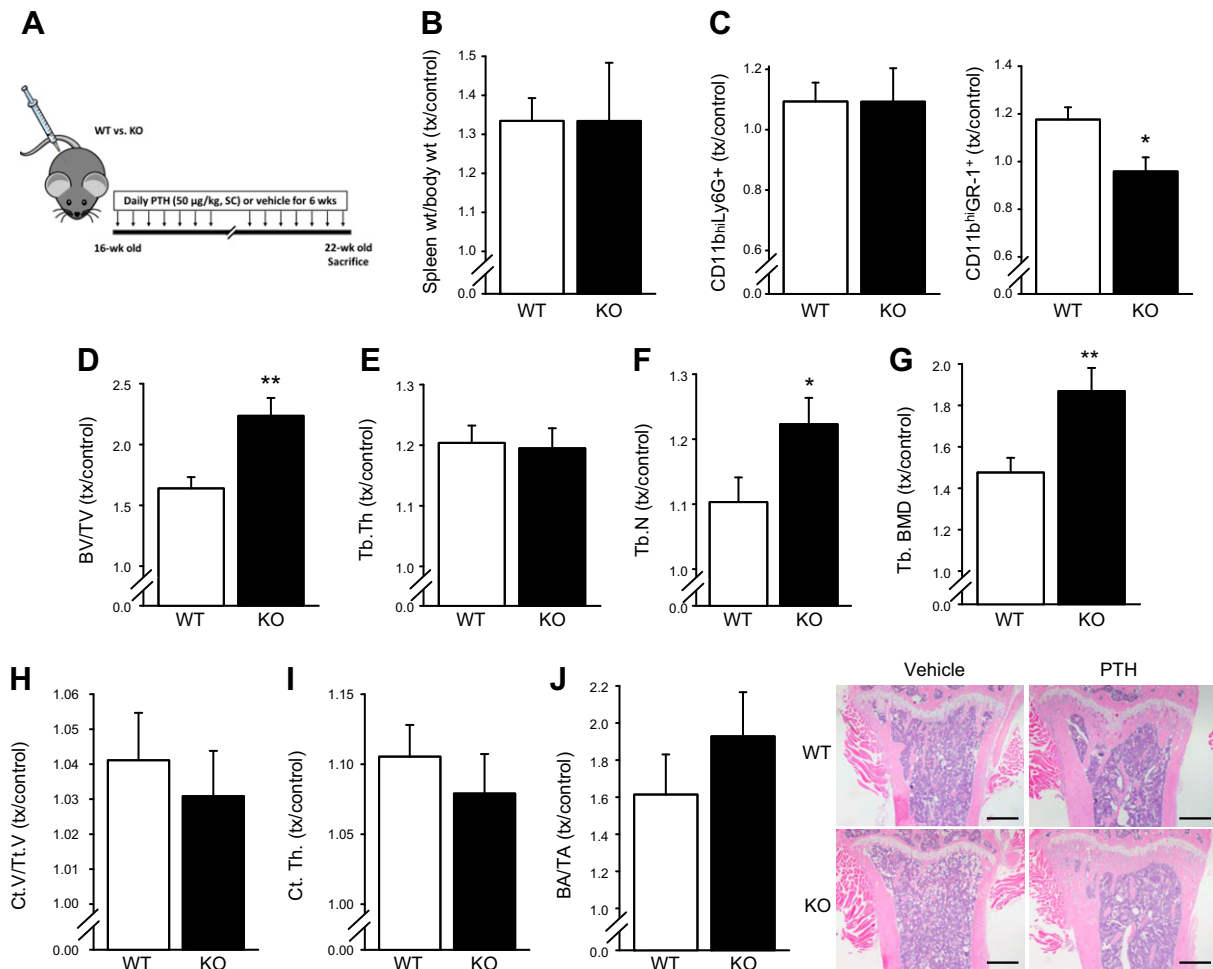
Figure 5. Anabolic response to PTH is greater in adult KO mice than WT. *A)* Experimental design. Daily injections of PTH (treatment, 50 μg/kg, s.c) were administered to female KO and WT mice (16 wk) or vehicle (control, 0.9% saline) for 6 wk and euthanized at 22 wk to assess spleen and marrow phenotypes. *B)* Spleens were harvested and weighed from vehicle and PTH-treated KO and WT mice. PTH treatment similarly increased spleen weight per body weight in both WT and KO mice (treatment: control >1.0). *C)* Marrow flow cytometric analysis for CD11b^{hi}Ly6G$^+$ and CD11b^{hi}Gr-1$^+$ populations showed that PTH treatment of WT mice resulted in increased CD11b^{hi}Gr-1$^+$ populations (treatment:control >1.0) but no change was seen in PTH-treated compared to vehicle-treated KO mice (treatment:control ~1.0). *D–G)* Trabecular analysis of proximal tibia *via* μCT. Both KO and WT displayed significantly increased BV/TV with PTH treatment. PTH treatment showed a greater anabolic effect in KO mice compared to WT. *H, I)* Cortical analysis of midshaft of tibia *via* μCT. WT and KO displayed increased cortical bone with PTH treatment. *J)* H&E-stained, paraffin-embedded sections of KO and WT tibiae treated with PTH or vehicle were quantified for bone area per total area. Both WT and KO mice had an anabolic response to PTH treatment (treatment:control >1.0). Scale bars, 500 μm. Data are means ± sem (n = 8–11/group). *$P < 0.05$, **$P < 0.01$.

overall decrease in the amount of bone that can be occupied by osteoclasts in the KO mice. Hence, less bone surface with more osteoclasts could translate into a reduction in serum TRAcP 5b. These data suggest that the reduced bone phenotype in 22-wk-old KO mice is in part related to an increase in osteoclasts on the bone surface. Proinflammatory cytokines increase osteoclastic differentiation and activity *via* upregulation of RANKL (32). Increased proinflammatory cytokine production has been associated with systemic and local bone loss in patients with inflammatory diseases (33, 34), including SLE (35), rheumatoid arthritis (36–38), inflammatory bowel disease (39, 40), and periodontal disease (41). Recombinant MFG-E8 protein decreased osteoclast differentiation, suggesting that MFG-E8 signaling directly affects pathways that participate in osteoclast differentiation and may be a

targeted treatment for inflammatory bone loss. These findings are similar to recently published articles detailing the contributions of MFG-E8 to osteoclast differentiation and function (14–16) and extend these findings into the inflammatory phenotype of an adult mouse model.

Macrophages have recently emerged as key regulators of bone homeostasis, yet the mechanisms by which they exert their effects are unclear (42, 43). Macrophages are phagocytic cells, and a distinct function of MFG-E8 is to act as a bridge between apoptotic cells and phagocytes to facilitate engulfment of dead cells (5). Accumulation of apoptotic cells leads to increased proinflammatory cytokine production. Polymorphisms of MFG-E8 have been found in cases of SLE, which is characterized by decreased apoptotic cell clearance, as well as decreased bone mass (44). The efferocytic capacity of splenic macrophages was

TABLE 1. *Complete blood counts*

Component	Unit	WT Veh (*n* = 10)	WT PTH (*n* = 11)	KO Veh (*n* = 10)	KO PTH (*n* = 10)
WBCs	10^3 cells/µl	4.7 ± 0.5	5.9 ± 0.6	4.7 ± 0.3	6.1 ± 0.6
NE	10^3 cells/µl	0.85 ± 0.10	0.91 ± 0.13	0.98 ± 0.11	0.96 ± 0.12
LY	10^3 cells/µl	3.7 ± 0.4	4.8 ± 0.4	3.6 ± 0.3	5.0 ± 0.5[‡]
MO	10^3 cells/µl	0.09 ± 0.01	0.11 ± 0.01	0.10 ± 0.02	0.10 ± 0.02
EO	10^3 cells/µl	0.03 ± 0.01	0.07 ± 0.02	0.05 ± 0.04	0.04 ± 0.01
BA	10^3 cells/µl	0.01 ± 0.004	0.03 ± 0.008	0.02 ± 0.01	0.01 ± 0.003
NE	%	18.1 ± 1.1	15.0 ± 0.9*	20.4 ± 1.4	15.5 ± 1.0[‡]
LY	%	79.0 ± 1.3	81.7 ± 1.1	76.3 ± 2.1	82.1 ± 1.0[‡]
MO	%	1.9 ± 0.3	2.0 ± 0.2	1.9 ± 0.2	1.7 ± 0.04
EO	%	0.65 ± 0.20	0.95 ± 0.29	0.95 ± 0.59	0.58 ± 0.18
BA	%	0.27 ± 0.06	0.38 ± 0.12	0.37 ± 0.20	0.14 ± 0.04
RBC	10^6 cells/µl	8.8 ± 0.1	8.5 ± 0.2	8.7 ± 0.1	7.8 ± 0.3[‡]
HB	g/dl	13.1 ± 0.2	12.7 ± 0.2	13.3 ± 0.1	12.3 ± 0.5
HCT	%	44.8 ± 0.9	43.9 ± 0.9	46.9 ± 0.7	43.0 ± 1.8
MCV	fl	50.8 ± 0.7	51.5 ± 0.5	53.9 ± 0.2[†]	55.2 ± 0.3[§]
MCH	pg	14.8 ± 0.2	15.0 ± 0.2	15.3 ± 0.1*	15.8 ± 0.1[‡]
MCHC	g/dl	29.2 ± 0.3	29.1 ± 0.3	28.4 ± 0.3	28.5 ± 0.2
RDW	%	17.1 ± 0.7	18.2 ± 0.1	16.0 ± 0.1	17.2 ± 0.1[¶]
PLT	10^3 cells/µl	747 ± 16	746 ± 22	744 ± 27	752 ± 14
MPV	fl	4.1 ± 0.06	4.1 ± 0.06	4.0 ± 0.03	4.0 ± 0.03

BA, basophil; EO, eosinophil; HB, hemoglobin; HCT, hematocrit; LY, lymphocyte; MCH, mean corpuscular hemoglobin; MCHC, mean corpuscular hemoglobin concentration; MCV, mean corpuscular volume; MO, monocyte; MPV, mean platelet volume; NE, neutrophil; PLT, platelet; RBC, red blood cell; RDW, red cell distribution width; WBCs, white blood cells. Data are expressed as means ± SEM. *$P < 0.05$ *vs.* WT Veh, [†]$P < 0.01$ *vs.* WT Veh, [‡]$P < 0.05$ *vs.* KO Veh, [§]$P < 0.01$ *vs.* KO Veh, and [¶]$P < 0.001$ *vs.* KO Veh.

suggested to be compromised by the increase in TUNEL^{+} cells; however, the efferocytic capacity of bone marrow macrophages was unchanged *in vitro* in MFG-E8–deficient mice. TUNEL[+] cell populations trended downward in the bone marrow whereas TUNEL staining of spleens, revealed increased apoptotic bodies in the white pulp of the spleen. This phenotype, consistent with previous literature (6), suggests that, *in vivo*, there is an alteration in apoptotic cell clearance in MFG-E8–deficient mice. The increase in TUNEL^{+} cells in MFG-E8–deficient spleens, but not the bone marrow, suggests compensatory efferocytic mechanisms are more operative and critical in the bone marrow environment. Alternatively, the data presented here that phagocytic functions of MFG-E8–deficient macrophages are compromised may suggest that MFG-E8 is important for macrophage clearance of debris or collagen fragments in bone *vs.* efferocytic clearance of apoptotic cells. Further, the increase in marrow neutrophils and MDSCs could reflect an altered phagocytic or efferocytic environment in the marrow. Ineffective efferocytosis leads to increased inflammatory cytokines that support the increase in these cells (45). Further understanding of the pathways that are most important in the marrow space will help delineate whether and how the process of apoptotic cell clearance regulates bone turnover.

The slow acquisition of the osteopenic phenotype in MFG-E8–deficient mice may be the product of age-related changes. Physiologic processes typically occur efficiently in young mice, whereas with age, the body has reduced efficiency of many physiologic processes that are associated with chronic elevation of proinflammatory cytokines. Age-associated inflammation has been termed "inflammaging" (46). Chronic inflammatory states support osteoclast differentiation and activity. The aging skeleton presents with increased osteoclast bone resorption relative to osteoblast formation, leading to a net reduction in bone (47, 48). The contributions of many inflammatory cytokines to age-associated osteoporosis have been studied and well characterized; however, the role of proresolution or anti-inflammatory cytokines are less well characterized. Given that MFG-E8 is a known anti-inflammatory mediator, its loss may lead to accelerated aging or inflammaging. Young mice may have the ability to compensate for the changes seen with MFG-E8 deficiency (*i.e.*, increased inflammatory milieu) whereas, adult mice may lose their ability to compensate for these changes and hence the effects of increased inflammation take hold.

MFG-E8 deficiency resulted in increased osteoclasts in association with an enhanced inflammatory environment in the murine skeleton (**Fig. 7**). Currently, therapeutic interventions for patients with inflammatory bone loss include antiresorptives, such as bisphosphonates, and anti-inflammatory targeted therapies. Intermittent PTH administration has been extensively studied for its anabolic effects in bone. Teriparatide [PTH(1-34)] is approved by the FDA, as mentioned earlier, but its use is limited to cases of severe osteoporosis. Recently, abaloparatide, which interacts with the same receptor as PTH, has received FDA approval (49). A better understanding of phenotypes in which PTH is a beneficial therapeutic could lead to more targeted use of anabolic agents.

In adult MFG-E8 KO mice, PTH was an effective therapeutic and resulted in a larger anabolic response in KO *vs.* WT mice. In addition, PTH treatment decreased the number of osteoclasts per bone surface in the adult KO
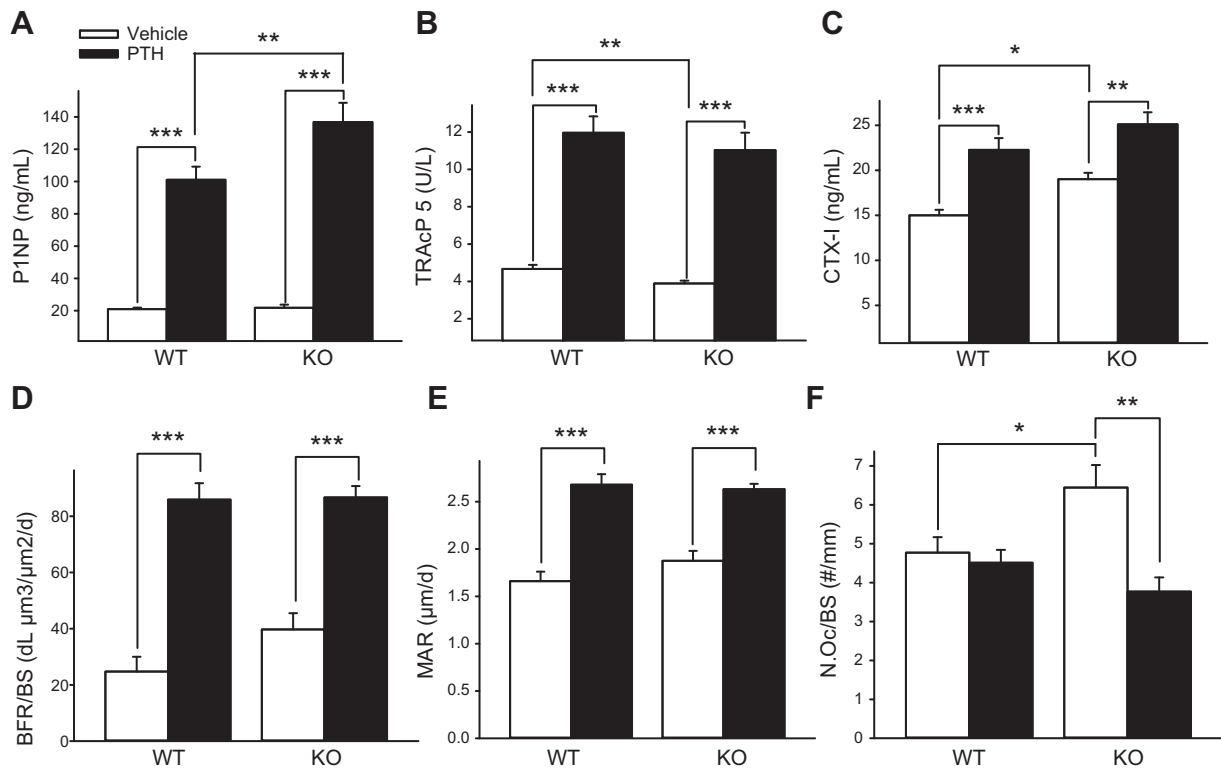
Figure 6. Bone formation and resorption analyses in PTH- and vehicle-treated KO and WT mice. *A–C*) Serum was collected at the time of euthanasia, and P1NP, TRAcP 5b, and CTX-I were measured *via* ELISA ($n = 10$–11/group). *D, E*) Calcein (30 mg/g, i.p.) was administered 5 and 2 d before euthanasia. Undecalcified tibiae were collected, fixed, and embedded, and sections were analyzed for BFR/BS and MAR. PTH treatment increased BFR/BS and MAR in both KO and WT. *F*) TRAP-stained, paraffin-embedded tibiae sections were quantified for TRAP+ multinucleated cells. KO mice treated with PTH showed decreased N.Oc/BS *vs.* vehicle-treated KO mice. Data are means ± SEM ($n = 8$–11/group). *$P < 0.05$, **$P < 0.01$, ***$P < 0.001$.

mice and brought the number of osteoclasts to the level of those in WT vehicle-treated mice. Treatment of mice with PTH has been shown to decrease peripheral neutrophils (22) and polymorphonuclear leukocyte infiltration in healing oral tissue (50). In our mouse model, PTH treatment similarly decreased the number of peripheral neutrophils. These data suggest that PTH therapy alters the inflammatory phenotype and is beneficial in the treatment of bone loss related to inflammation. PTH increases specialized proresolving factors in the bone marrow including resolvin D1 and D2 and lipoxins, suggesting that PTH therapy aids in the resolution of inflammation (51). A study of the application of PTH in a murine model of rheumatoid arthritis showed that PTH
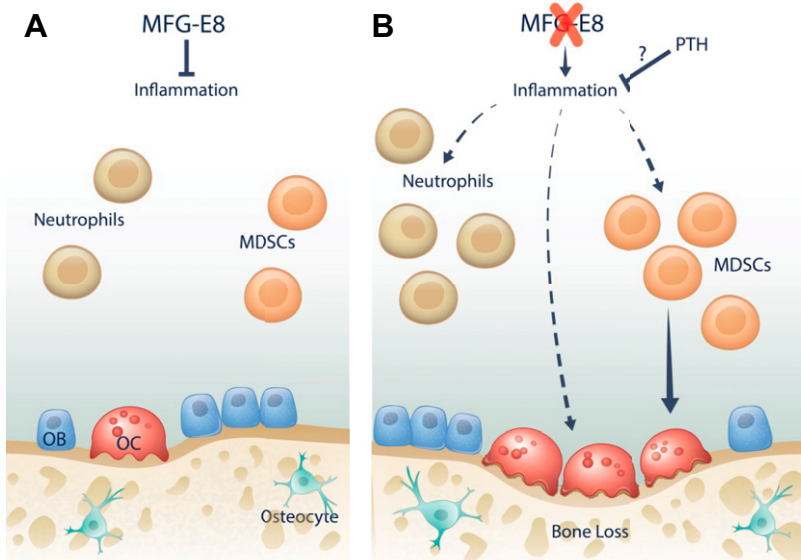
Figure 7. *A*) In WT mice, MFG-E8 is present and functional. Aberrant inflammation is minimal and osteoclastogenesis, osteoclast activity, and bone mass are at baseline levels. *B*) With MFG-E8 deficiency, inflammation increases, causing an increase in neutrophils and MDSCs, a subset of myeloid cells that can differentiate into osteoclasts. Increased inflammatory cytokines lead to increased osteoclastogenesis and osteoclast activity, resulting in decreased bone mass. When PTH is administered to MFG-E8–deficient mice, inflammation is reduced and osteoclastogenesis is decreased, leading to an increase in bone mass.

repaired local erosions (52). In addition, a human clinical trial showed that the teriparatide increased bone mass in patients with rheumatoid arthritis (53), and a clinical trial of local PTH application to periodontal defects showed enhanced bone regeneration in PTH-treated lesions (54). Collectively, these data suggest that PTH is an effective therapeutic in certain types of inflammatory bone disease, yet future studies are necessary to confirm the breadth of its therapeutic benefit.

These findings are of interest to the bone and immunology fields, but our study is not without its limitations. Mouse models are not perfect tools to study human disease, and future studies are needed to enhance the translational elements of these findings. Isolation of tissue samples from patients with autoimmune diseases should be tested for MFG-E8 activity. In addition, clinical trials using the FDA-approved teriparatide in autoimmune patients who are susceptible to decreased bone mass may shed light on future expanded uses of teriparatide and the more newly approved abaloparatide.

In summary, our data show that MFG-E8 deficiency leads to an altered immunologic profile in the murine bone marrow, is associated with bone loss with age, and is highly responsive to intermittent PTH therapy. [FJ]

AUTHOR CONTRIBUTIONS

M. N. Michalski and L. K. McCauley designed the study; M. N. Michalski, A. L. Seydel, E. M. Siismets, L. E. Zweifler, A. J. Koh, and B. P. Sinder, performed the research; M. N. Michalski, A. L. Seydel, E. M. Siismets, L. E. Zweifler, and J. I. Aguirre collected and analyzed the data; M. N. Michalski and L. K. McCauley wrote the manuscript; and all authors revised and approved the manuscript.

REFERENCES

1. Atabai, K., Fernandez, R., Huang, X., Ueki, I., Kline, A., Li, Y., Sadatmansoori, S., Smith-Steinhart, C., Zhu, W., Pytela, R., Werb, Z., and Sheppard, D. (2005) Mfge8 is critical for mammary gland remodeling during involution. *Mol. Biol. Cell* **16**, 5528–5537
2. Atabai, K., Jame, S., Azhar, N., Kuo, A., Lam, M., McKleroy, W., Dehart, G., Rahman, S., Xia, D. D., Melton, A. C., Wolters, P., Emson, C. L., Turner, S. M., Werb, Z., and Sheppard, D. (2009) Mfge8 diminishes the severity of tissue fibrosis in mice by binding and targeting collagen for uptake by macrophages. *J. Clin. Invest.* **119**, 3713–3722
3. Kudo, M., Khalifeh Soltani, S. M., Sakuma, S. A., McKleroy, W., Lee, T. H., Woodruff, P. G., Lee, J. W., Huang, K., Chen, C., Arjomandi, M., Huang, X., and Atabai, K. (2013) Mfge8 suppresses airway hyperresponsiveness in asthma by regulating smooth muscle contraction. *Proc. Natl. Acad. Sci. USA* **110**, 660–665
4. Nandrot, E. F., Anand, M., Almeida, D., Atabai, K., Sheppard, D., and Finnemann, S. C. (2007) Essential role for MFG-E8 as ligand for alphavbeta5 integrin in diurnal retinal phagocytosis. *Proc. Natl. Acad. Sci. USA* **104**, 12005–12010
5. Hanayama, R., Tanaka, M., Miwa, K., Shinohara, A., Iwamatsu, A., and Nagata, S. (2002) Identification of a factor that links apoptotic cells to phagocytes. *Nature* **417**, 182–187
6. Hanayama, R., Tanaka, M., Miyasaka, K., Aozasa, K., Koike, M., Uchiyama, Y., and Nagata, S. (2004) Autoimmune disease and impaired uptake of apoptotic cells in MFG-E8-deficient mice. *Science* **304**, 1147–1150
7. DeCathelineau, A. M., and Henson, P. M. (2003) The final step in programmed cell death: phagocytes carry apoptotic cells to the grave. *Essays Biochem.* **39**, 105–117
8. Ravichandran, K. S., and Lorenz, U. (2007) Engulfment of apoptotic cells: signals for a good meal. *Nat. Rev. Immunol.* **7**, 964–974
9. Uchiyama, A., Yamada, K., Ogino, S., Yokoyama, Y., Takeuchi, Y., Udey, M. C., Ishikawa, O., and Motegi, S. (2014) MFG-E8 regulates angiogenesis in cutaneous wound healing. *Am. J. Pathol.* **184**, 1981–1990
10. Soki, F. N., Koh, A. J., Jones, J. D., Kim, Y. W., Dai, J., Keller, E. T., Pienta, K. J., Atabai, K., Roca, H., and McCauley, L. K. (2014) Polarization of prostate cancer-associated macrophages is induced by milk fat globule-EGF factor 8 (MFG-E8)-mediated efferocytosis. *J. Biol. Chem.* **289**, 24560–24572
11. Kusunoki, R., Ishihara, S., Aziz, M., Oka, A., Tada, Y., and Kinoshita, Y. (2012) Roles of milk fat globule-epidermal growth factor 8 in intestinal inflammation. *Digestion* **85**, 103–107
12. Aziz, M. M., Ishihara, S., Mishima, Y., Oshima, N., Moriyama, I., Yuki, T., Kadowaki, Y., Rumi, M. A., Amano, Y., and Kinoshita, Y. (2009) MFG-E8 attenuates intestinal inflammation in murine experimental colitis by modulating osteopontin-dependent alphavbeta3 integrin signaling. *J. Immunol.* **182**, 7222–7232
13. Hu, C. Y., Wu, C. S., Tsai, H. F., Chang, S. K., Tsai, W. I., and Hsu, P. N. (2009) Genetic polymorphism in milk fat globule-EGF factor 8 (MFG-E8) is associated with systemic lupus erythematosus in human. *Lupus* **18**, 676–681
14. Sinningen, K., Albus, E., Thiele, S., Grossklaus, S., Kurth, T., Udey, M. C., Chavakis, T., Hofbauer, L. C., and Rauner, M. (2015) Loss of milk fat globule-epidermal growth factor 8 (MFG-E8) in mice leads to low bone mass and accelerates ovariectomy-associated bone loss by increasing osteoclastogenesis. *Bone* **76**, 107–114
15. Albus, E., Sinningen, K., Winzer, M., Thiele, S., Baschant, U., Hannemann, A., Fantana, J., Tausche, A. K., Wallaschofski, H., Nauck, M., Völzke, H., Grossklaus, S., Chavakis, T., Udey, M. C., Hofbauer, L. C., and Rauner, M. (2016) Milk fat globule-epidermal growth factor 8 (MFG-E8) is a novel anti-inflammatory factor in rheumatoid arthritis in mice and humans. *J. Bone Miner. Res.* **31**, 596–605
16. Abe, T., Shin, J., Hosur, K., Udey, M. C., Chavakis, T., and Hajishengallis, G. (2014) Regulation of osteoclast homeostasis and inflammatory bone loss by MFG-E8. *J. Immunol.* **193**, 1383–1391
17. Matsuda, A., Jacob, A., Wu, R., Zhou, M., Nicastro, J. M., Coppa, G. F., and Wang, P. (2011) Milk fat globule-EGF factor VIII in sepsis and ischemia-reperfusion injury. *Mol. Med.* **17**, 126–133
18. Miksa, M., Wu, R., Dong, W., Komura, H., Amin, D., Ji, Y., Wang, Z., Wang, H., Ravikumar, T. S., Tracey, K. J., and Wang, P. (2009) Immature dendritic cell-derived exosomes rescue septic animals via milk fat globule epidermal growth factor-factor VIII [corrected]. *J. Immunol.* **183**, 5983–5990
19. Das, A., Ghatak, S., Sinha, M., Chaffee, S., Ahmed, N. S., Parinandi, N. L., Wohleb, E. S., Sheridan, J. F., Sen, C. K., and Roy, S. (2016) Correction of MFG-E8 resolves inflammation and promotes cutaneous wound healing in diabetes. *J. Immunol.* **196**, 5089–5100
20. Isogai, Y., Akatsu, T., Ishizuya, T., Yamaguchi, A., Hori, M., Takahashi, N., and Suda, T. (1996) Parathyroid hormone regulates osteoblast differentiation positively or negatively depending on the differentiation stages. *J. Bone Miner. Res.* **11**, 1384–1393
21. Schiller, P. C., D'Ippolito, G., Roos, B. A., and Howard, G. A. (1999) Anabolic or catabolic responses of MC3T3-E1 osteoblastic cells to parathyroid hormone depend on time and duration of treatment. *J. Bone Miner. Res.* **14**, 1504–1512
22. Novince, C. M., Michalski, M. N., Koh, A. J., Sinder, B. P., Entezami, P., Eber, M. R., Pettway, G. J., Rosol, T. J., Wronski, T. J., Kozloff, K. M., and McCauley, L. K. (2012) Proteoglycan 4: a dynamic regulator of skeletogenesis and parathyroid hormone skeletal anabolism. *J. Bone Miner. Res.* **27**, 11–25

23. Cho, S. W., Soki, F. N., Koh, A. J., Eber, M. R., Entezami, P., Park, S. I., van Rooijen, N., and McCauley, L. K. (2014) Osteal macrophages support physiologic skeletal remodeling and anabolic actions of parathyroid hormone in bone. *Proc. Natl. Acad. Sci. USA* **111**, 1545–1550

24. Chang, M. K., Raggatt, L. J., Alexander, K. A., Kuliwaba, J. S., Fazzalari, N. L., Schroder, K., Maylin, E. R., Ripoll, V. M., Hume, D. A., and Pettit, A. R. (2008) Osteal tissue macrophages are intercalated throughout human and mouse bone lining tissues and regulate osteoblast function in vitro and in vivo. *J. Immunol.* **181**, 1232–1244

25. Bouxsein, M. L., Boyd, S. K., Christiansen, B. A., Guldberg, R. E., Jepsen, K. J., and Müller, R. (2010) Guidelines for assessment of bone microstructure in rodents using micro-computed tomography. *J. Bone Miner. Res.* **25**, 1468–1486

26. Sinder, B. P., Zweifler, L., Koh, A. J., Michalski, M. N., Hofbauer, L. C., Aguirre, J. I., Roca, H., and McCauley, L. K. (2017) Bone mass is compromised by the chemotherapeutic trabectedin in association with effects on osteoblasts and macrophage efferocytosis. *J. Bone Miner. Res.* **32**, 2116–2127

27. Dempster, D. W., Compston, J. E., Drezner, M. K., Glorieux, F. H., Kanis, J. A., Malluche, H., Meunier, P. J., Ott, S. M., Recker, R. R., and Parfitt, A. M. (2013) Standardized nomenclature, symbols, and units for bone histomorphometry: a 2012 update of the report of the ASBMR Histomorphometry Nomenclature Committee. *J. Bone Miner. Res.* **28**, 2–17

28. Cho, S. W., Pirih, F. Q., Koh, A. J., Michalski, M., Eber, M. R., Ritchie, K., Sinder, B., Oh, S., Al-Dujaili, S. A., Lee, J., Kozloff, K., Danciu, T., Wronski, T. J., and McCauley, L. K. (2013) The soluble interleukin-6 receptor is a mediator of hematopoietic and skeletal actions of parathyroid hormone. *J. Biol. Chem.* **288**, 6814–6825

29. Miksa, M., Komura, H., Wu, R., Shah, K. G., and Wang, P. (2009) A novel method to determine the engulfment of apoptotic cells by macrophages using pHrodo succinimidyl ester. *J. Immunol. Methods* **342**, 71–77

30. Odell, W. D., and Heath III, H. (1993) Osteoporosis: pathophysiology, prevention, diagnosis, and treatment. *Dis. Mon.* **39**, 789–867

31. Neutzner, M., Lopez, T., Feng, X., Bergmann-Leitner, E. S., Leitner, W. W., and Udey, M. C. (2007) MFG-E8/lactadherin promotes tumor growth in an angiogenesis-dependent transgenic mouse model of multistage carcinogenesis. *Cancer Res.* **67**, 6777–6785

32. Redlich, K., and Smolen, J. S. (2012) Inflammatory bone loss: pathogenesis and therapeutic intervention. *Nat. Rev. Drug Discov.* **11**, 234–250

33. Mundy, G. R. (2007) Osteoporosis and inflammation. *Nutr. Rev.* **65**, S147–S151

34. Romas, E., and Gillespie, M. T. (2006) Inflammation-induced bone loss: can it be prevented? *Rheum. Dis. Clin. North Am.* **32**, 759–773

35. García-Carrasco, M., Mendoza-Pinto, C., Escárcega, R. O., Jiménez-Hernández, M., Etchegaray Morales, I., Munguía Realpozo, P., Rebollo-Vázquez, J., Soto-Vega, E., Delezé, M., and Cervera, R. (2009) Osteoporosis in patients with systemic lupus erythematosus. *Isr. Med. Assoc. J.* **11**, 486–491

36. Gough, A. K., Lilley, J., Eyre, S., Holder, R. L., and Emery, P. (1994) Generalised bone loss in patients with early rheumatoid arthritis. *Lancet* **344**, 23–27

37. Roldán, J. F., Del Rincón, I., and Escalante, A. (2006) Loss of cortical bone from the metacarpal diaphysis in patients with rheumatoid arthritis: independent effects of systemic inflammation and glucocorticoids. *J. Rheumatol.* **33**, 508–516

38. Gravallese, E. M., Harada, Y., Wang, J. T., Gorn, A. H., Thornhill, T. S., and Goldring, S. R. (1998) Identification of cell types responsible for bone resorption in rheumatoid arthritis and juvenile rheumatoid arthritis. *Am. J. Pathol.* **152**, 943–951

39. Paganelli, M., Albanese, C., Borrelli, O., Civitelli, F., Canitano, N., Viola, F., Passariello, R., and Cucchiara, S. (2007) Inflammation is the main determinant of low bone mineral density in pediatric inflammatory bowel disease. *Inflamm. Bowel Dis.* **13**, 416–423

40. Ali, T., Lam, D., Bronze, M. S., and Humphrey, M. B. (2009) Osteoporosis in inflammatory bowel disease. *Am. J. Med.* **122**, 599–604

41. Yoshihara, A., Seida, Y., Hanada, N., and Miyazaki, H. (2004) A longitudinal study of the relationship between periodontal disease and bone mineral density in community-dwelling older adults. *J. Clin. Periodontol.* **31**, 680–684

42. Michalski, M. N., and McCauley, L. K. (2017) Macrophages and skeletal health. *Pharmacol. Ther.* **174**, 43–54

43. Sinder, B. P., Pettit, A. R., and McCauley, L. K. (2015) Macrophages: their emerging roles in bone. *J. Bone Miner. Res.* **30**, 2140–2149

44. Panopalis, P., and Yazdany, J. (2009) Bone health in systemic lupus erythematosus. *Curr. Rheumatol. Rep.* **11**, 177–184

45. Korns, D., Frasch, S. C., Fernandez-Boyanapalli, R., Henson, P. M., and Bratton, D. L. (2011) Modulation of macrophage efferocytosis in inflammation. *Front. Immunol.* **2**, 57

46. Franceschi, C., Bonafè, M., Valensin, S., Olivieri, F., De Luca, M., Ottaviani, E., and De Benedictis, G. (2000) Inflamm-aging. An evolutionary perspective on immunosenescence. *Ann. N. Y. Acad. Sci.* **908**, 244–254

47. Gordan, G. S., and Genant, H. K. (1985) The aging skeleton. *Clin. Geriatr. Med.* **1**, 95–118

48. Syed, F. A., and Ng, A. C. (2010) The pathophysiology of the aging skeleton. *Curr. Osteoporos. Rep.* **8**, 235–240

49. Shirley, M. (2017) Abaloparatide: first global approval. *Drugs* **77**, 1363–1368

50. Kuroshima, S., Mecano, R. B., Tanoue, R., Koi, K., and Yamashita, J. (2014) Distinctive tooth-extraction socket healing: bisphosphonate versus parathyroid hormone therapy. *J. Periodontol.* **85**, 24–33

51. McCauley, L. K., Dalli, J., Koh, A. J., Chiang, N., and Serhan, C. N. (2014) Cutting edge: parathyroid hormone facilitates macrophage efferocytosis in bone marrow via proresolving mediators resolvin D1 and resolvin D2. *J. Immunol.* **193**, 26–29

52. Redlich, K., Görtz, B., Hayer, S., Zwerina, J., Doerr, N., Kostenuik, P., Bergmeister, H., Kollias, G., Steiner, G., Smolen, J. S., and Schett, G. (2004) Repair of local bone erosions and reversal of systemic bone loss upon therapy with anti-tumor necrosis factor in combination with osteoprotegerin or parathyroid hormone in tumor necrosis factor-mediated arthritis. *Am. J. Pathol.* **164**, 543–555

53. Ebina, K., Hashimoto, J., Shi, K., Kashii, M., Hirao, M., and Yoshikawa, H. (2014) Comparison of the effect of 18-month daily teriparatide administration on patients with rheumatoid arthritis and postmenopausal osteoporosis patients. *Osteoporos. Int.* **25**, 2755–2765

54. Bashutski, J. D., Eber, R. M., Kinney, J. S., Benavides, E., Maitra, S., Braun, T. M., Giannobile, W. V., and McCauley, L. K. (2010) Teriparatide and osseous regeneration in the oral cavity. *N. Engl. J. Med.* **363**, 2396–2405